ISSN 2616-5872 Vol.6, Issue 5: 57-72, DOI: 10.25236/AJEE.2024.060509

A study of tropospheric multi-pollutants and their relationship dynamics in the Middle East

Tianzhen Ju[1,2,a,*], Zhichao Lv[1,2,b], Bingnan Li[3,c], Lanzhi Wang[1,2,d], Zhenrong Gu[1,2,e]

[1]College of Geography and Environmental Sciences, Northwest Normal University, Lanzhou, China
[2]The Key Laboratory of Resource Environment and Sustainable Development of Oasis, Lanzhou, Gansu Province, China
[3]News and Mass Communication Department, Shaanxi Normal University, Xi'an, 710062, China
[a]jutianzhen@nwnu.edu.cn, [b]2760679951@qq.com, [c]iambingcita@sina.com, [d]1780415246@qq.com, [e]1271079696@qq.com
[*]Corresponding author

Abstract: *Due to the harsh natural environmental conditions in the Middle East and the fact that ozone is one of the top pollutants, research on ozone and its related pollutants has become more relevant in the countries concerned. This research is based on diverse datasets from the OMI instrument and utilizes backward trajectory analysis as well as Pearson spatial correlation to analyze the relationships between primary pollutant control zones during the warm seasons from 2010 to 2020 in the Middle East and meteorological factors. Research findings reveal the following.1. In terms of spatial distribution, ozone is primarily concentrated in the northwestern and central regions of the Middle East, while formaldehyde is predominantly found in the northern part of the region. Nitrogen dioxide, on the other hand, is mainly distributed in the northeastern portion of the Middle East. 2. In terms of time, ozone has shown a fluctuating upward trend since 11 years, with ozone considerably higher in summer than in winter; formaldehyde shows a higher winter than summer; and nitrogen dioxide shows a normal distribution. In order to facilitate environmental management, this study conducts an analysis of ozone-sensitive control areas within the research area at both annual and monthly scales. Results show that at the annual scale, ozone sensitivity is characterized by mixed or transitional control zones, while at the monthly scale, various control types are predominant.3. An analysis of the chemical and climatic processes involved in the formation of ozone showed a significant positive correlation between ozone and nitrogen dioxide, and an uncorrelated and weakly negative correlation with formaldehyde; ozone was positively correlated with temperature, and significantly negatively correlated with barometric pressure and relative humidity.4. Research on the HYSPLIT model and Weighted Potential Source Contribution Function for the elevated ozone regions in the Middle East indicates that the transport pathways of ozone pollution are primarily composed of two main components: the Persian Gulf and the Mediterranean.*

Keywords: *the Middle East, Tropospheric Ozone, OMI, Trend analysis*

1. Introduction

Tropospheric ozone sources can be categorized into anthropogenic and natural sources, with anthropogenic sources comprising the majority. The ozone generated from anthropogenic sources primarily originates from the production and combustion of fossil fuels, as well as automobile exhaust emissions (Li et al., 2023)[1][2]. However, the natural sources mainly refer to the portion that is imported from the stratosphere to the troposphere (Cristofanelli P. et al. 2010)[3]. The continued accumulation of volatile organic compounds (VOCs) and nitrogen oxides (NO_X), among the precursors of ozone, can lead to the formation of photochemical smog and ozone under certain conditions.

In recent years, the projected concentration levels of tropospheric ozone are increasing globally and are considerably regionalized (Ziemke. et al. 2019)[4]. With the elevated rate of economic development in the Middle East, industrialization and urbanization have increased proportionately. This is accompanied by strong anthropogenic emissions leading to an increase in the concentration of atmospheric pollutants (Lelieveld. et al.2016)[5], such as the elevation of column densities of volatile organic compounds (VOCs) and nitrogen oxides (NO_X).

Moreover, the unique meteorological conditions in the Middle East, including intense solar radiation,

ISSN 2616-5872 Vol.6, Issue 5: 57-72, DOI: 10.25236/AJEE.2024.060509

elevated temperatures, and arid climate, contribute to making the region one of the fewer hospitable areas for human habit from both natural and societal perspectives (Tadic et al., 2020)[6]. Therefore, academic interest in the issue of ozone pollution in the Middle East has been steadily growing. Atifa Nadeem et al. (2024) used multi-satellite remote sensing data to quantify springtime aerosols over Saudi Arabia over a lengthy period of time and obtained that the two main aerosol subtypes, i.e., absorbing mixed aerosols and neutral fine particles, are considered to be dominant in the Kingdom of Saudi Arabia[7]. Al Suwaidi, A. al. (2024) used United Arab Emirates air monitoring stations and PM10 data to derive that in desert countries such as the UAE, seasonal variations in PM10 column densities are closely related to seasonal variations in heat waves and dust storms, which are characteristic of dryland climates[8]. During the summer months, the UAE experiences elevated temperatures and drought conditions that create favorable conditions for the formation of heat waves.

In response to the problem of ozone pollution, scholars in the Middle East have also conducted some studies. In their study, Jiang et al. (2016) employed the GEOS-Chem model and NOx emissions data to specifically quantify the impact of regional emissions on summer ozone levels in the Middle East. The research highlights that the enhancement of ozone in the mid-troposphere during the Middle East summer is primarily attributed to NOx emissions from Asia, with these NOx emissions originating mainly from anthropogenic activities and lightning[9]. Ozone pollutants in the lower troposphere in the Middle East region mainly result from lightning-generated NOx from Europe and North America and NOx emissions from local anthropogenic sources in the Middle East[10]. Zohdirad, H. et al. (2022) investigated the chemical coupling of NO, NO_2, and O_3 using backward trajectory clustering analysis and found that the atmospheric oxidizing capacity is higher in Tehran compared to the rest of the world. Ozone levels in Tehran are likely influenced by local source regions of pollutants, with air masses from the eastern and northeastern regions contributing the most to O_3 pollution, while air masses from the western regions represent the most distant pathways for the increase in O_3 levels[11].

As the economic resources of the Middle East region are mainly dependent on energy exports, the Middle East region accounts for 48.67% of the global oil reserves. The Middle East has a large number of oil fields, and the process of oil production produces a certain amount of exhaust gases such as dust, carbon monoxide, nitrogen oxides, sulfur dioxide, and other pollutants. These pollutants exhibit characteristics such as complex composition, elevated toxicity, diversity, concentrated emissions, and significant harm, which consequently contribute to severe air pollution issues in the region[12][13].

However, the spatial distribution, temporal dynamics, multi-pollutant species spatial relationships, migration paths and dynamics of ozone and other multi-pollutants in the Middle East are less reported. In this paper, the spatial distribution, temporal dynamics, spatial relationship of multi-pollutants, migration paths and dynamics of multi-pollutants in the Middle East are investigated based on the multivariate data of OMI using backward trajectory and Pearson's spatial correlation methods.

2. Overview of the study area

The Middle East is located in Europe, Asia, Africa, the combination of three continents, most of the region in the 15 ° N ~ 40 ° N, and bordered by the Arabian Sea, the Red Sea, the Mediterranean Sea, the Black Sea, the Caspian Sea, but also communicates with the Atlantic Ocean and the Indian Ocean.

The primary climatic types in this region are tropical desert, Mediterranean, and temperate continental climates. Among these, the tropical desert climate is the most widespread, characterized by its location under the influence of subtropical high pressure and the dry northeast winds from arid inland regions of Asia. Annual precipitation in this climate zone is less than 500 millimeters, with average temperatures ranging from 20 to 30 degrees Celsius, and daylight hours exceeding 2000 hours, resulting in a predominantly arid and low-rainfall environment.

The ecological environment in the Middle East region is extremely complex and diverse. The area encompasses a variety of geographical features, including deserts, mountains, coastal plains, and lakes. Furthermore, a significant portion of the region lies at elevations ranging from 0 to 1000 meters above sea level, contributing to considerable variations in vegetation types across the Middle East. This diverse topography and geography have a substantial impact on the ecological diversity and landscapes found in the region. Vegetation types in the Middle East vary considerably depending on climatic conditions. Desert regions in the Middle East are primarily characterized by desert vegetation, which includes cacti, shrubs, and grassland plants. In contrast, coastal areas and mountainous regions tend to have more lush and diverse vegetation, such as palm trees, olive trees, and oak trees.

ISSN 2616-5872 Vol.6, Issue 5: 57-72, DOI: 10.25236/AJEE.2024.060509

The Middle East region comprises a total of 20 countries and territories, including Saudi Arabia, Iran, Iraq, Kuwait, the United Arab Emirates, Oman, Qatar, Bahrain, Turkey, Israel, Palestine, Syria, Lebanon, Jordan, Yemen, Cyprus, Georgia, Armenia, Azerbaijan, and Egypt. These nations collectively have a population of approximately 490 million people, as shown in Figure 1.

The Middle East region has been a transportation hub between the East and the West since ancient times, and is the land of "two oceans, three continents and five seas", with an extremely significant strategic position and valuable natural resources, such as oil and natural gas, etc., of which 26 percent of the world's oil reserves in the Middle East are in the world's largest oil market.

However, in recent years, they have also been challenged by numerous environmental problems, such as land desertification, water scarcity, air pollution, and ecological damage[14].

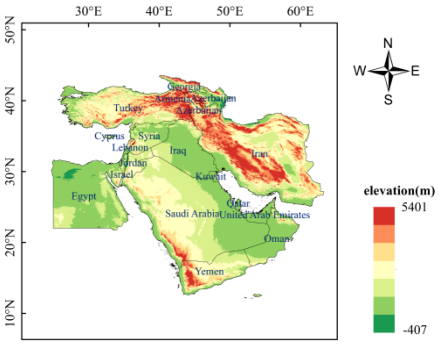

Figure 1: Overview of the Middle East study area

3. Date and research methods

3.1. Data sources

Daily data on atmospheric ozone column densities (here tropospheric ozone column densities) in the Middle East from 2010 to 2020 provided by OMI on board the Aura satellite were used in this study. The data have a spatial resolution of 13 km × 24 km, a sensor field of view of 114°, a wavelength range of 270 to 500 nm, an average spectral resolution of 0.5 nm, and a swath width of 2,600 km. These data were downloaded from the Goddard Center for Earth Science Data and Information Services on the official website of NASA and stored in HDF5 format. Various types of meteorological data information of the study area were obtained from the National Science and Technology Resources Sharing Service Platform of the National Earth System Science Data Center of China. The DEM (Digital Elevation Model, DEM) was produced using the SRTM (Shuttle Radar Topography Mission, SRTM) Digital Terrain Elevation Model (DTEM) data package.

3.2. Research methodology

This study initially acquired daily remote sensing tropospheric ozone concentration data for the Middle East region spanning from 2010 to 2020. Subsequently, Python software was employed to extract latitude, longitude, ozone concentration, and cloud cover data. To ensure precision in boundary extraction, an expanded boundary range was selected.

The processing process is then carried out using Python programming language and Arcgis 10.8 software and other operations. Based on the results obtained, the obtained data were plotted in Arcgis 10.8 to produce spatial and temporal distribution maps of tropospheric ozone concentration in the Middle East for different time scales.

Ozone generation sensitivity analysis is a spatial and temporal variation method to classify ozone sensitivity by analyzing the ratio of formaldehyde to nitrogen dioxide (FNR). In conjunction with the findings of Wang et al. (2021), a threshold for ozone sensitivity control ($HCHO/NO_2$) was determined[15]. The results were categorized as follows: areas where the ratio of $HCHO/NO_2$ is less than 2.3 were designated as VOC control zones, areas where the ratio falls between 2.3 and 4.2 were categorized as mixed control zones, and areas where the ratio exceeds 4.2 were identified as NO_X control zones.

ISSN 2616-5872 Vol.6, Issue 5: 57-72, DOI: 10.25236/AJEE.2024.060509

The Pearson correlation calculation method is an indicator applied to the degree of correlation between two variables. Its range of variation falls between -1 and 1. In conjunction with the research findings of Peng et al. (2022), the method was used to analyze the relationship between tropospheric ozone concentration and formaldehyde, nitrogen dioxide, and meteorological factors[16]. The calculation formula is:

$$r_{xy} = \frac{\sum_{i=1}^{n}\left[\left(x_i - \bar{x}\right)\left(y_i - \bar{y}\right)\right]}{\sqrt{\sum_{i=1}^{n}\left(x_i - \bar{x}\right)^2 \sum_{i=1}^{n}\left(y_i - \bar{y}\right)^2}} \tag{1}$$

where rxy's is the correlation coefficient between x and y, with values between [-1,1]; xi denotes the mean value of ozone column density in month i; yi denotes the mean value of meteorological factors in year i; denotes the annual mean ozone column density; denotes the annual mean value of meteorological factors; and n is the number of samples.

The Potential Source Contribution Function (PSCF), also known as the Residence Time Analysis, is a method that divides the study period's airflow trajectory coverage area into grid cells based on the fundamental principle of conditional probability functions to identify potential pollution source locations. In this study, ozone daily data were integrated with GDAS meteorological data, and the Potential Source Contribution Function (PSCF) was employed to investigate the transport pathways and potential source distribution at representative locations in the Middle East. The calculation formula for PSCF analysis is as shown in Equation (2):

$$\mathrm{PSCF}\ (\mathrm{i,j}) = \frac{m_{(i,j)}}{n_{(i,j)}} \tag{2}$$

Where PSCF（i,j）is the percentage of specific airflow trajectories in each grid; m(i,j) is the number of contaminated trajectory nodes passing through in the grid (i,j), and n(i,j) is the total number of trajectory nodes passing in grid (i,j). In order to reduce the effect of uncertainty caused by the small n(i,j) in grid (i,j), the PSCF should be weighted by the factor W(i,j). W(i,j) is the number of air mass trajectory nodes in the grid. The empirical weight values are determined, and the weights are set as shown in (3) in this paper:

$$W(i,j) = \begin{cases} 1.0, 80 > n(i,j) \\ 0.70, 20 < n(i,j) \le 80 \\ 0.42, 10 < n(i,j) \le 20 \\ 0.05, 0 < n(i,j) \le 10 \end{cases} \tag{3}$$

The PSCF is weighted to derive the WPSCF value, and the WPSCF calculation formula is shown in Equation (4):

$$\mathrm{WPSCF(i,j)=W(i,j)\times PSCF(i,j)} \tag{4}$$

Where WPSCF(i,j) denotes the potential area of the pollutant, the higher the corresponding WPSCF value, the more trajectory nodes passing through the grid area, the greater the potential contribution to the pollutant mass concentration in the study area.

4. Results and analysis

4.1. Annual average spatial distribution of tropospheric ozone, formaldehyde and nitrogen dioxide column densities in the Middle East, 2010-2020

Figure 2 illustrates the spatial distribution of ozone, formaldehyde, and nitrogen dioxide concentration data based on OMI for the years 2010 to 2020. Figure 2 (a) shows that spatially, ozone is significantly affected by topography[17]. Elevated ozone column densities are observed in the northern regions of Egypt, most of Iraq, and along the western coast of the Persian Gulf. In the northern part of Egypt, ozone column densities even exceed 41.3 DU. Conversely, ozone column densities are lower in Yemen and Iran, with the southern part of Yemen having column densities below 34.7 DU. The general spatial distribution pattern of ozone in the study area shows higher column densities in the northwestern

ISSN 2616-5872 Vol.6, Issue 5: 57-72, DOI: 10.25236/AJEE.2024.060509

and central regions, and lower column densities in the northeastern and southwestern regions. Over the 11-year period, ozone distribution remained relatively stable, with minor interannual variations in pollution levels.

The spatial distribution of formaldehyde concentration, as depicted in Figure 2 (b), displays a latitudinal pattern in the Middle East region. Elevated formaldehyde column densities are found in the northern part of the Middle East region and a tiny section in the southern part of Yemen. Areas such as Azerbaijan, Georgia, and the western region of Turkey have formaldehyde column densities exceeding 13.2×10^{15}molec/cm^2. Lower formaldehyde values are observed near the Saudi Arabia-Yemen border and in the southern part of Egypt, with column densities in these areas falling below 7.8×10^{15}molec/cm^2. Transitional zones are present in different regions.

Figure 2 (c) shows the spatial distribution of nitrogen dioxide concentration in the Middle East region. Elevated nitrogen dioxide column densities are primarily located along the coast of the Persian Gulf and the southeastern coast of the Mediterranean. In these areas, nitrogen dioxide column densities reach levels exceeding 4.4×10^{15}molec/cm^2. Conversely, low column densities of nitrogen dioxide are observed in the southern part of the Middle East region and the southern region of Egypt, where column densities are below 4.4×10^{15}molec/cm^2. Transitional zones are also present in different areas.

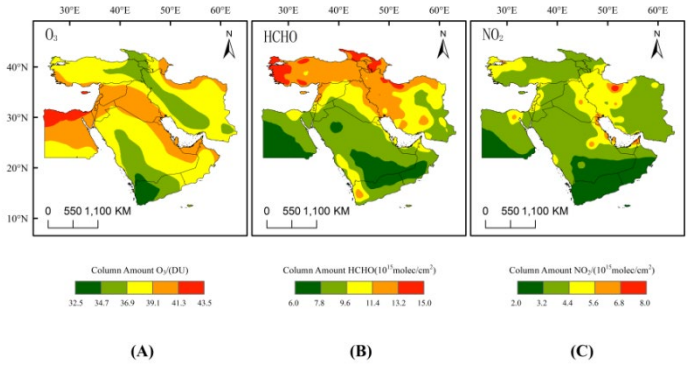

Figure 2: Spatial distribution of mean tropospheric column density column densities of ozone, formaldehyde and nitrogen dioxide in the Middle East for the 11-year period 2010-2020

4.2. Monthly and annual spatial and temporal distribution of tropospheric ozone in the Middle East region

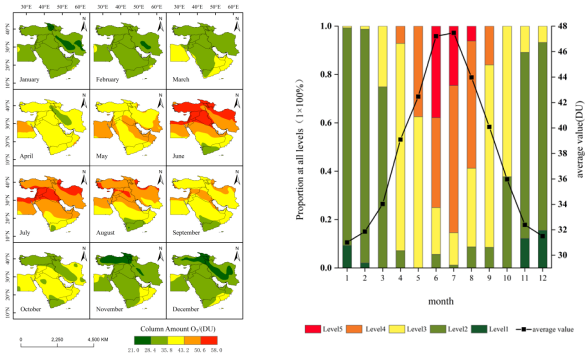

Figure 3 (a): Monthly spatial distribution of O_3 column densities in the Middle East for 11 years
Figure 3 (b): Changes in the share of different classes of O_3 column densities and monthly average values in the Middle East in 11 years

The monthly mean spatial distribution of ozone column densities in the Middle East is divided into five tiers Figure 3 (a), Level 1: 21.0-28.4; Level 2: 28.4-35.8; Level 3: 35.8-43.2; Level 4: 43.2-50.6; and Level 5: 50.6-58.0. Monthly spatial distributions of ozone are classified using April and September as classification nodes, respectively: April-September The monthly spatial distribution of ozone in the Middle East can be divided into two categories: Between April and September, the Middle East exhibits a distribution pattern of ozone concentration with lower values in the southern regions and higher values in the northern regions. During this period, ozone column densities fall within the range of 39 to 50 DU,

ISSN 2616-5872 Vol.6, Issue 5: 57-72, DOI: 10.25236/AJEE.2024.060509

with ozone levels primarily categorized as level four to level five. In contrast, during the six months from October to March (1 to 6), the region displays a distribution pattern with lower ozone column densities in the southern parts and higher column densities in the northern parts. Ozone column densities during these months typically range from 30 to 40 DU, with ozone levels primarily categorized as level one to level three.

Over the course of these 12 months, from January to June, ozone pollution column densities gradually increase. In June, the central Middle East regions, such as Iraq and Syria, reach ozone column densities classified as level five, covering approximately 38% of the Middle East's total area. From July to December, ozone column densities gradually decrease. In July, the ozone levels are classified as level five in the northern regions, level four in the middle regions, and level three in the southern regions. In August, these levels reduce to level four, level three, and level two, and by September, they drop further to include some level four and level three regions as well as a substantial presence of level two. In October, the tropospheric ozone concentration is exclusively categorized as level three and level two. In November and December, ozone column densities begin to increase from the northern regions of the Middle East. By March, a pattern emerges with higher ozone column densities in the southeastern parts of Egypt and the Arabian Peninsula, while the central and northern regions exhibit lower column densities. Consequently, ozone levels in the Middle East exhibit significant seasonal variations, with ozone column densities during the summer months decreasing from north to south, and during the winter months increasing from north to south[18].

Figure 3 (b) illustrates that ozone concentration follows a normal distribution pattern. Elevated ozone column densities are concentrated in the months from April to September, while from October to the following March, ozone column densities are consistently lower. In other words, ozone column densities in the summer months are significantly higher than those in the winter months. The highest monthly average ozone concentration in the Middle East region, as well as in China, is observed in July. In the Middle East, it reaches 47 DU, while in the Beijing-Tianjin-Hebei region and Liaoning province of China, it is 42 DU. The lowest monthly average ozone concentration in the Middle East is recorded in January, with a value of 31 DU. The difference between the highest and lowest monthly values is 16 DU.

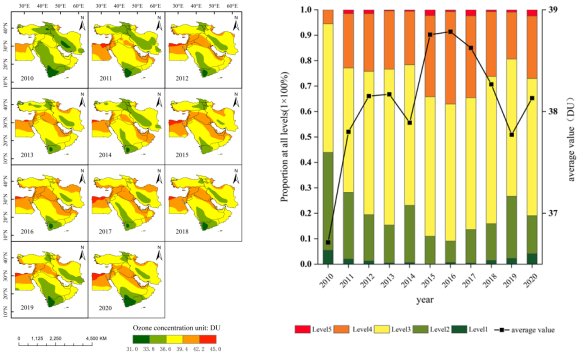

Figure 4 (a): Inter-annual variation of O_3 column densities in the Middle East for 11 years Figure 4 (b): Changes in the share of different classes and annual average of O_3 column densities in the Middle East in 11 years

The 11-year annual average ozone column densities in the Middle East can be categorized into the following five tiers Figure.4 (a), Level 1: 31.0 to 33.8; Level 2: 33.8 to 36.6; Level 3: 36.6 to 39.4; Level 4: 39.4 to 42.2; and Level 5: 42.2 to 45.0.

Figure 4 (a) shows that the extreme Middle East ozone column densities are distributed in the central part of the Middle East region, mainly in the two regions of northern Egypt and the west coast of the Persian Gulf. The lowest values occur in Yemen, with additional areas forming a transition zone. Among these 11 years, the ozone concentration in 2010 was relatively low.

Figure 4 (b) illustrates the percentage distribution of annual average ozone column densities across the five levels for the 11-year period. During this time frame, the most predominant level of ozone concentration in the Middle East is level three, accounting for approximately 54% of the total, followed by level four at 23%. The highest ozone column densities in the region were recorded in 2015 and 2016, with level four accounting for 32% and 36%, respectively. The ozone column densities during these years were 38.76 DU and 38.78 DU.

In the decade from 2011 to 2020, areas with elevated levels of ozone concentration V are found every

ISSN 2616-5872 Vol.6, Issue 5: 57-72, DOI: 10.25236/AJEE.2024.060509

year. From 2010 to 2016, the percentage of level two ozone concentration areas decreased annually, with the exception of a significant increase in the percentage of level two areas in 2014, reaching 29%. Ozone column densities in 2014 were 37.89 DU, higher than in 2013. In 2015, the Middle East showed a sharp increase in ozone concentration, with an increase of 2% compared to 2014. From 2016 to 2020, the ozone secondary occupancy region increased every year, with the largest increase in the ozone secondary occupancy region in 2019, with an increase of 50% compared to 2018; the ozone concentration was 37.77 DU. Overall, over the past 11 years, ozone column densities in the Middle East have displayed some degree of periodicity and largely exhibited an increasing trend.

4.3. Monthly mean spatial and temporal distribution of formaldehyde in the troposphere in the Middle East region

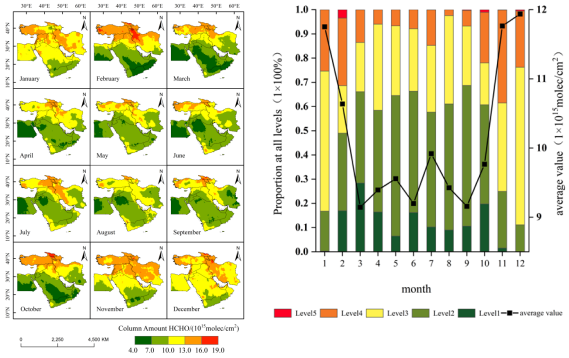

Figure 5 (a): Monthly spatial distribution of HCHO column densities in the Middle East for 11 years
Figure 5 (b): Changes in the share of different classes and monthly average of HCHO concentration in the Middle East in 11 years

The monthly average spatial distribution of formaldehyde in the Middle East is divided into five tiers Figure 5 (a), Level 1: 4.0-7.0; Level 2: 7.0-10.0; Level 3: 10.0-13.0; Level 4: 13.0-16.0; and Level 5: 16.0-19.0.

Monthly average spatial distributions of formaldehyde column densities are categorized into two classes using March and October as the classification nodes, respectively: between March and October, formaldehyde column densities formed a low distribution in the center and a elevated distribution in the south and north of Saudi Arabia. The spatial distribution of HCHO concentration from March to October exhibits a pattern where central areas have lower column densities, while the northern and southern regions of Saudi Arabia and Yemen experience higher column densities. During this period, HCHO column densities range between 9 to 10×10^{15}molec/cm^2, with levels one to three being predominant. In contrast, from November to February, there is a pattern of lower column densities in the south and higher column densities in the north. During this time, HCHO column densities range between $10\sim12\times10^{15}$molec/cm^2, with levels three to five being predominant.

During these 12 months, the formaldehyde concentration showed a sharp downward trend from January to March, and in February, the formaldehyde concentration in the northwestern part of Iran rose to level 5, with the range of level 5 accounting for about 3.5% of the area of the Middle East. From April to October, HCHO column densities fluctuate only slightly. In November and December, HCHO column densities gradually increase in the northern part of the Middle East, resulting in a distribution pattern with higher column densities in the north and lower column densities in the south. In general, HCHO column densities are positively correlated with vegetation indices. Hence, regions with higher vegetation indices, such as Georgia and Armenia in the northern part of the Middle East, exhibit higher HCHO column densities, while the southern part of the Middle East has lower HCHO column densities. The distribution patterns of HCHO column densities in both summer and winter follow a decreasing trend from north to south. Since HCHO is influenced by factors such as vegetation, population, economic activity, precipitation, and temperature differences between different regions[19], the differences in tropospheric HCHO column densities between the two Middle Eastern seasons, characterized by elevated temperatures and minor human activity, are relatively tiny.

Figure 5 (b) presents an overall "U"-shaped pattern for HCHO column densities in the Middle East. Elevated HCHO column densities are concentrated in the months from November to February, while from March to October, HCHO column densities are consistently low. The highest HCHO concentration

ISSN 2616-5872 Vol.6, Issue 5: 57-72, DOI: 10.25236/AJEE.2024.060509

in the Middle East is recorded in December at 11.9×10^{15}molec/cm^2, while the lowest concentration is in September at 9.2×10^{15}molec/cm^2. In the Beijing-Tianjin-Hebei region of China, the highest HCHO concentration is observed in June, reaching 14×10^{15}molec/cm^2. The difference between the highest and lowest monthly values in the Middle East is 2.7×10^{15}molec/cm^2.

4.4. Monthly mean spatial and temporal distribution of tropospheric nitrogen dioxide in the Middle East region

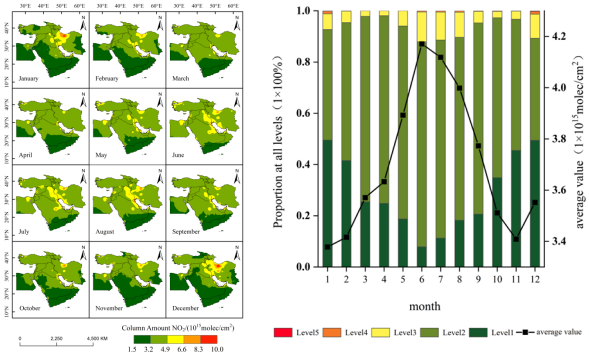

Figure 6 (a): Monthly spatial distribution of NO_2 column densities in the Middle East for 11 years
Figure 6 (b) :Changes in the share of different classes and monthly means of NO_2 column densities in the Middle East in 11 years

The monthly average spatial distribution of NO_2 column densities in the Middle East was categorized into five tiers Figure 6 (a), Level 1: 1.5 to 3.2; Level 2: 3.2 to 4.9; Level 3: 4.9 to 6.6; Level 4: 6.6 to 8.3; and Level 5: 8.3 to 10.0.

Figure 6 (a) illustrates that NO_2 column densities in the Middle East exhibit a pattern with elevated levels along the western coast of the Persian Gulf and lower levels in the rest of the region. Notably, regions with the highest NO_2 column densities are observed in January, October, and December. From April to September, NO_2 column densities in the Middle East range between 3.6 and 4.2×10^{15}molec/cm^2, whereas during October, November, December, January, February, and March, column densities range from 3 to 3.6×10^{15}molec/cm^2.

In general, NO_2 column densities are higher in the regions along the coast of the Persian Gulf and the southeastern Mediterranean coast, while the southern part of the Middle East experiences lower NO_2 column densities. Several factors contribute to this pattern, including low humidity, a significant number of oilfields, and a dense population, resulting in higher anthropogenic traffic-related NO_2 emissions. Additionally, the geographic location of the Persian Gulf, situated between the Zagros Mountains and the Arabian Plateau, limits the diffusion of NO_2 over a relatively tiny area. Therefore, NO_2 column densities in the Middle East are slightly higher in the summer compared to the winter months[20].

From January to June, NO_2 column densities in the Middle East exhibit a gradual upward trend, with NO_2 column densities in June being predominantly in level five, accounting for approximately 80% of the region. From July to November, NO_2 column densities gradually decrease, with December showing a 35% increase compared to November. Figure 6 (b) shows that the nitrogen dioxide concentration in the Middle East shows a single peak. It can be seen that the elevated values of nitrogen dioxide concentration are concentrated from April to September, while the nitrogen dioxide concentration is low from October to March. The highest concentration of nitrogen dioxide in the Middle East was 4.17×10^{15}molec/cm^2 in June, and the lowest monthly concentration was 3.38×10^{15}molec/cm^2 in January, while the highest monthly concentration in the Beijing-Tianjin-Hebei region of China was 6×10^{15}molec/cm^2 in December. The difference between the highest and the lowest monthly average values in the Middle East was 0.79×10^{15}molec/cm^2.

4.5. Sensitivity analysis of ozone generation in the Middle East

Based on the satellite data of OMI tropospheric formaldehyde concentration and nitrogen dioxide concentration in the Middle East from 2010 to 2020, an analysis of the spatial distribution and temporal trends of ozone precursors and ozone sensitivity categories (VOC control, mixed or transitional control, NO_X control) was conducted. This analysis aims to provide a theoretical basis for environmental

ISSN 2616-5872 Vol.6, Issue 5: 57-72, DOI: 10.25236/AJEE.2024.060509

management[21].

Figure 7 (a) shows the spatial distribution of ozone-sensitive control areas in the Middle East from 2010 to 2020, from which it can be seen that the spatial distribution of ozone-sensitive control areas in the Middle East varies considerably from year to year.

During the years 2010 to 2020, most regions in the Middle East were primarily categorized as ozone-sensitive mixed or transitional control areas. From 2010 to 2017, the majority of Saudi Arabia, countries along the eastern Mediterranean coast, Tehran in Iran, and Hama in Oman were classified as ozone-sensitive VOC control areas for most of the time. Starting in 2018, a shift occurred in the Middle East, with mixed or transitional control areas becoming predominant in most regions and a reduction in VOC control areas. However, in the same year, ozone-sensitive NOx control areas emerged in the vicinity of Sanaa in Yemen. This distribution pattern aligns with the findings of previous studies by William et al. (2014) and Barkley et al. (2017).

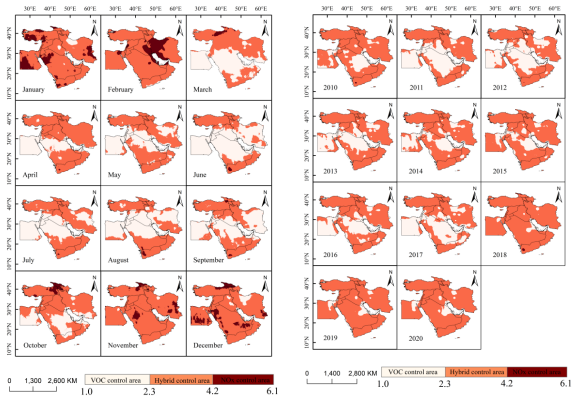

Figure 7 (a): Spatial distribution of O_3 sensitive control areas in the Middle East for 11 years
Figure 7 (b): Monthly spatial distribution of O_3 sensitive control areas in the Middle East

Figure 7 (b) displays the monthly spatial distribution of ozone-sensitive control areas in the Middle East. From the figure, it is evident that the monthly distribution of ozone-sensitive control areas in the Middle East exhibits significant variations. In general, for the months of January and February, most regions in the Middle East are characterized by a predominant presence of mixed or transitional control areas. In January, parts of western Egypt, southwestern Turkey, northwestern Saudi Arabia, and eastern Iran fall under the category of NOx control areas. However, in February, the regions classified as NOx control areas shift to central Iran. From March to October, the Middle East is primarily characterized by mixed or transitional control areas along with VOC control areas. In this period, there is a decrease in VOC control areas in April and May, followed by an increase in VOC control areas from June to September. VOC control areas are concentrated mainly in countries such as Saudi Arabia, Egypt, and Iran during these months. The Middle East is dominated by mixed or transitional control areas, and VOC control areas in April and May. In April and May, VOC-controlled areas in the Middle East decreased, and then increased from June to September, with VOC-controlled areas concentrated in Saudi Arabia, Egypt, and Iran, etc[22]. From October to December, the Middle East gradually recovered to be dominated by mixed or transitional control areas, and NOx-controlled areas appeared in northeastern Turkey and Georgia, and NOx-controlled areas appeared in the area around Medina, Saudi Arabia, in the same period[23].

4.6. Ozone correlation analysis

This study mainly analyzes the effects of tropospheric (A, a) formaldehyde concentration, (B, b) nitrogen dioxide concentration, and temperature, barometric pressure, and relative humidity on ozone concentration in the Middle East. In this paper, the correlation coefficients are categorized into eight levels: -1 to -0.75 strong negative correlation, -0.75 to -0.5 moderate negative correlation, -0.5 to -0.25 weak negative correlation, -0.25 to 0 (and 0 to 0.25) uncorrelated, 0.25 to 0.5 weak positive correlation, 0.5 to 0.75 moderate positive correlation, and 0.75 to 1 strong positive correlation. Figure 8 illustrates the spatial correlations and P-value distributions between ozone concentration and the column densities of formaldehyde and nitrogen dioxide over an 11-year period in the Middle East[24][25].

ISSN 2616-5872 Vol.6, Issue 5: 57-72, DOI: 10.25236/AJEE.2024.060509

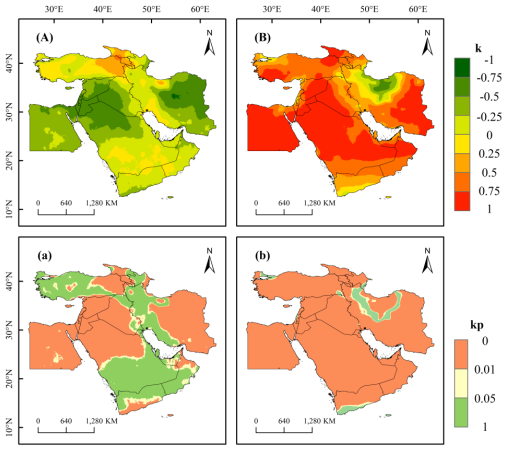

Figure 8: Spatial correlation between O_3 concentration and (A, a) HCHO concentration, (B, b) NO_2 concentration in the Middle East for the year 11

As can be seen in (A, a) of Figure 8, the correlation coefficients between ozone and formaldehyde column densities ranged from -0.78 to 0.56, and the regions with P-values less than 0.05 accounted for about 63.5% of the total region, mainly in Egypt, the central region of the Middle East, and the western part of Iran. Approximately 63.5% of the regions have P-values less than 0.05. These regions are primarily distributed in Egypt, the central Middle East, and western Iran, with some presence in Turkey and Yemen. In the Middle East, the relationship between ozone concentration and formaldehyde concentration is mainly characterized by no correlation or weak negative correlation, with these two categories accounting for about 80.4% of the total area. Moreover, in most areas within these categories, the P-values are less than 0.05. This phenomenon is due to the fact that formaldehyde is a precursor for ozone production, and some formaldehyde is consumed in the process of ozone formation, so that uncorrelated and weakly negatively correlated areas are formed.

As can be seen from (B, b) in Figure 8, the correlation coefficients between ozone concentration and nitrogen dioxide concentration range from -0.71 to 0.91 with a P-value of less than 0.05, and account for about 96.9% of the total area, which is distributed over the vast majority of the Middle East, except for a minor portion of the southern part of Yemen and the areas of Sanandaj, Kermanshah, and Tabriz in Iran. The Middle East is dominated by regions with moderate and strong positive correlation between ozone concentration and nitrogen dioxide concentration, which together account for about 70.1% of the total region. This phenomenon is likely due to the fact that nitrogen dioxide is also a precursor to ozone generation. In the Middle East, the presence of numerous oil fields and continuous emissions from traffic contribute to nitrogen dioxide production. Moreover, the heavy atmospheric dispersion, influenced by the topography of elevated terrain on both sides and lower terrain in the middle of the Middle East, results in the accumulation of nitrogen dioxide, thus forming a moderate to strong positive correlation.

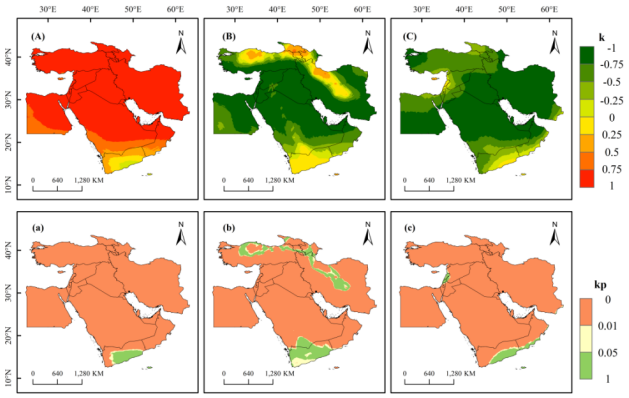

Figure 9: Spatial correlation between O_3 concentration and (A, a) air temperature, (B, b) air pressure, and (C, c) relative humidity in the Middle East for year 11

Figure 9 shows the spatial correlation between (A, a) air temperature, (B, b) air pressure, (C, c) relative humidity and ozone concentration in the Middle East for 11 years and the distribution of P-

ISSN 2616-5872 Vol.6, Issue 5: 57-72, DOI: 10.25236/AJEE.2024.060509

values[26]. From (A, a) in Figure 9, it can be seen that the correlation coefficients between ozone concentration and temperature range from -0.10 to 0.94, and the regions with P-values less than 0.05 account for about 97.8% of the total region, which is distributed over the vast majority of the Middle East, except for a tiny portion of the southern part of Yemen. The Middle East region is dominated by a strong positive correlation between ozone concentration and temperature, which accounts for about 82.8% of the total region. Moreover, in most regions within this category, the P-values are less than 0.05. This positive correlation can be attributed to the fact that under conditions of elevated temperature and strong solar radiation[27], photochemical reactions intensify, leading to an increase in ozone concentration, thus forming a region of strong positive correlation[28].

Figure 9 (B, b) reveals that the correlation coefficients between ozone concentration and pressure range from -0.92 to 0.56. Approximately 90.3% of the regions have P-values less than 0.05, with exceptions in some areas surrounding the Persian Gulf in Iran, the vicinity of Bandar Abbas, Turkey's Ankara, and Georgia, among others. Ozone concentration and barometric pressure in the Middle East are dominated by regions of moderate negative correlation and strong negative correlation, which together account for about 75.6% of the total region. This phenomenon may be due to the weakening of surface atmospheric pressure, which, in turn, leads to an increase in temperature favoring ozone generation. Conversely, when surface atmospheric pressure increases, it is frequently accompanied by windy weather, reducing photochemical reactions and hindering ozone concentration. This results in the observed medium to strong negative correlations.

In Figure 9 (C, c), the correlation coefficients between ozone concentration and relative humidity range from -0.93 to 0.45. About 97.5% of the regions exhibit P-values less than 0.05, with exceptions in some areas in the southern parts of Yemen, Oman, and Lebanon. Ozone concentration and relative humidity in the Middle East are dominated by regions of moderate negative correlation and strong negative correlation, which together account for about 88.5% of the total region. Humidity also affects ozone concentration to a certain extent. Under high humidity conditions, ozone undergoes light extinction due to the formation of an absorption mechanism under the influence of water vapor, reducing solar radiation intensity. Additionally, elevated humidity leads to substantial ozone consumption during atmospheric photochemical reactions, further reducing ozone concentration. Conversely, lower humidity and higher temperatures favor ozone concentration, resulting in the observed medium to strong negative correlations[29].

4.7. Middle East based on HYSPLIT model and WPSCF analysis

Due to adverse meteorological conditions such as low wind and temperature inversions, atmospheric pollutants tend to accumulate, leading to more severe air pollution events. This study employed Meteoinfo software and the TrajStat plugin to conduct backward trajectory simulations and cluster analysis of air masses. The trajectory backtracking time was set at 24 hours, and the trajectory simulation height was 500 meters, which can accurately reflect the movement characteristics of the atmospheric boundary layer airflow. This approach allows for the examination of the distribution and extent of pollutant transport from external sources.

The study focused on three research locations in the Middle East, namely Riyadh, Saudi Arabia (24.70°N, 46.70°E), Tel Aviv, Israel (32.07°N, 34.77°E), and Abu Dhabi, United Arab Emirates (24.47°N, 54.37°E). These locations represent the central, northeastern, and southwestern high-value areas in the Middle East. The analysis was conducted seasonally, with each season yielding four transport pathways at each location. The study also considered daily ozone concentration data corresponding to each location's specific timeframes to explore the transport pathways and potential source distribution of ozone.

From Figure 10 (a), it is evident that during the summer season, the predominant transport direction for Riyadh, Saudi Arabia, is towards the northeast (36.61%), with this pathway mainly covering areas within Saudi Arabia. It primarily passes through the northern regions of the Eastern Province and the northeastern parts of Riyadh Province. Overall, the main transport direction during the summer is toward the northeast, accounting for 69.4% of the total, and it consistently traverses domestic territories, including the Eastern Province and Riyadh Province. Based on the WPSCF values, it can be seen that the potential source area of Riyadh in summer is dominated by local sources, followed by the cities of Khufufu, Majma'a, and Haf al-Abbatin, which do not contribute significantly to ozone. In contrast, during the winter season, the most significant proportion of transport pathways for Riyadh is directed towards the southeast (34.46%), covering areas primarily within Saudi Arabia. It passes through the southern regions of the Eastern Province and the eastern parts of Riyadh Province. Overall, the main transmission direction in winter is southeast with 61.58% and it passes through the Eastern Province and the eastern

ISSN 2616-5872 Vol.6, Issue 5: 57-72, DOI: 10.25236/AJEE.2024.060509

part of Riyadh Province. The spatial distribution of WPSCF values shows that the winter ozone in Riyadh is dominated by local sources, followed by the northern part of the Eastern Province and the area around Riyadh city.

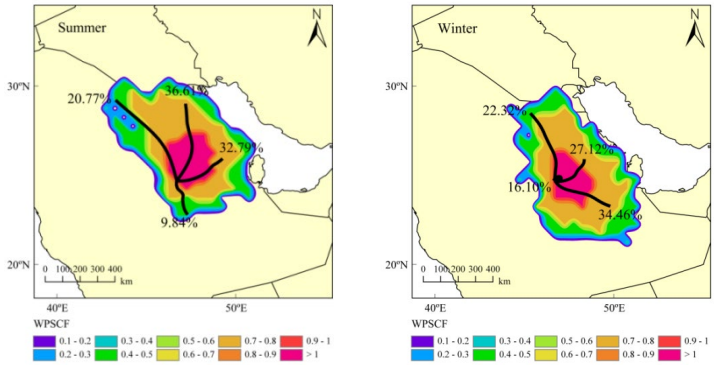

Figure 10 (a): O_3 transport paths and potential source areas for different seasons in Riyadh, 2019-2020

Figure 10 (b). presents the distribution of ozone transport pathways and potential source areas in Tel Aviv, Israel, during different seasons in 2019-2020. The figure reveals that during the summer season, the primary ozone transport direction for Tel Aviv is towards the northwest, accounting for a proportion of 68.58%, and predominantly traverses the coastal regions of the eastern Mediterranean Sea. Analyzing the WPSCF values, it becomes evident that during the summer season in Tel Aviv, the potential source areas are primarily influenced by local sources, with a significant impact from the coastal regions of the eastern Mediterranean along the summer transport pathways. Additionally, the influence of external transport from Lebanon and Cyprus should not be disregarded. In contrast, during the winter season, the largest proportion of ozone transport pathways for Tel Aviv is directed southwestward, constituting 32.05%. Most of this transport pathway passes through foreign territories, including Palestine and Jordan. Overall, the main transport direction in winter is the north-west with 49.59% and it passes through the eastern coast of the Mediterranean Sea, while the longest transport air mass is from the Mediterranean-Egyptian border, which represents the air mass with faster wind speeds. The potential source areas in Tel Aviv mainly behave in winter as in summer. The spatial distribution of WPSCF values shows that winter ozone in Tel Aviv is also dominated by local sources, and additional exogenous transport does not differ from summer[30].

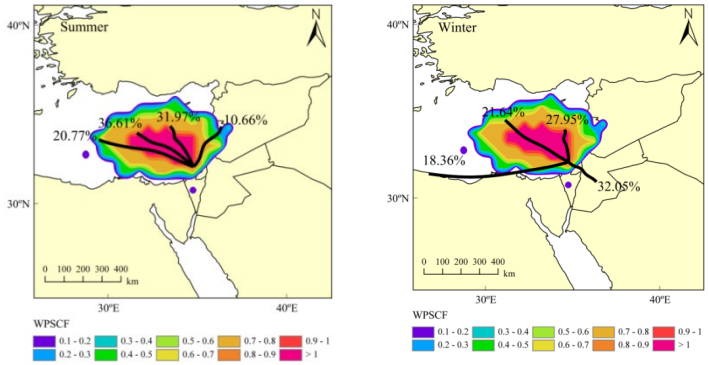

Figure 10 (b): O_3 transport paths and potential source areas for different seasons in Tel Aviv, 2019-2020

The transmission paths and potential sources of ozone in the United Arab Emirates were analyzed using Abu Dhabi as a representative point, as shown in Figure 10 (c). From the figure, it can be seen that the main transmission direction in Abu Dhabi during the summer months is north-west with a share of 84.7%, which mainly passes through most of the Persian Gulf. However, in terms of individual transmission paths, the northern path with the largest share is 33.61% and it mainly passes through the southern part of the Persian Gulf. The southwestern path has the smallest share of 15.3% and passes through the United Arab Emirates proper and northern Oman. According to the WPSCF values, the potential source area of Abu Dhabi in summer is dominated by local sources, followed by transmission from the Persian Gulf region. In winter, the main transmission direction in Abu Dhabi is northeast with

ISSN 2616-5872 Vol.6, Issue 5: 57-72, DOI: 10.25236/AJEE.2024.060509

a percentage of 38.36%, which mainly passes through the Persian Gulf near the coast of the United Arab Emirates. The southwestern transport path increased compared to summer with a percentage of 21.64%. From the WPSCF values, it can be seen that the potential source area in Abu Dhabi in winter is similar to that in summer, which is also dominated by local sources, but the concentration of potential sources in winter tends to migrate to the east compared to that in summer.

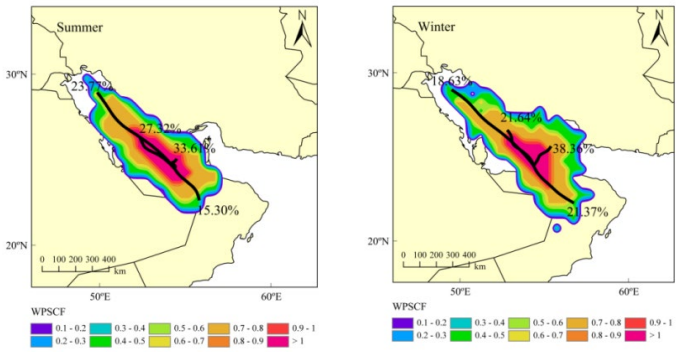

Figure 10 (c): O_3 transport paths and potential source areas for different seasons in Abu Dhabi, 2019-2020

5. Conclusions

1) The spatial distribution of ozone and precursors in the Middle East region varies, with a strong spatial distribution pattern in the northwest and center of the region and a low distribution pattern in the northeast and southwest, with the elevated value areas mainly located in northern Egypt, most of Iraq, and the west coast of the Persian Gulf. Overall there is a significant difference in the spatial distribution, and the distribution of ozone is more stable in the high and low value areas. As a precursor of ozone, formaldehyde is distributed longitudinally, with high values in the northern part of the Middle East and a tiny part of the southern part of Yemen, while nitrogen dioxide is distributed more stably, with high values in the Persian Gulf coast and the southeastern coast of the Mediterranean Sea. In terms of temporal distribution, high ozone values are mainly observed from April to September, and this distribution pattern is similar to nitrogen dioxide. However, the distribution of formaldehyde shows an opposite seasonal variation.2) On an annual scale, most of the Middle East is dominated by ozone-sensitive mixing or transition control areas. However, on a monthly scale, the control and management of ozone pollution also adopts a "one-month policy" to reduce ozone production by increasing humidity on urban roads during hot periods.3) The Pearson correlation analysis reveals that ozone and nitrogen dioxide are significantly positively correlated, while ozone and formaldehyde show no significant correlation or a weak negative correlation. Ozone is positively correlated with temperature but negatively correlated with pressure and relative humidity.4) Based on the analysis of ozone transport pathways and potential sources in the Middle East, it is evident that Riyadh, Saudi Arabia, exhibits westward transport pathways in both summer and winter, with local sources being the primary contributors, followed by contributions from the Eastern Province. Abu Dhabi, United Arab Emirates, also displays west-northwest transport pathways in both seasons, with ozone potential source areas primarily local and located around the Persian Gulf. Tel Aviv, Israel, shows northeastward transport pathways in both summer and winter, with local sources being the primary contributors, particularly along the west coast of the Mediterranean Sea. Therefore, enhancing control over emissions from transportation and industrial sources can help reduce local contributions and collaboration with neighboring regions to jointly mitigate ozone pollution.

Statements and Declarations

Funding This work was funded by Lanzhou Science and Technology Plan Project (2017-RC-69) and the National Natural Science Foundation of China (2016YFC0500907) at the Key Laboratory of Resource Environment and Sustainable Development of Oasis, Gansu province, and the Gansu Province Environmental Science and Engineering Demonstration Laboratory.

Author Contributions

Tianzhen Ju: methodology, writing-original draft, writing—review and editing, data curation,

ISSN 2616-5872 Vol.6, Issue 5: 57-72, DOI: 10.25236/AJEE.2024.060509

resources, visualization, formal analysis.

Zhichao Lv: project administration, conceptualization, writing—review and editing, methodology, supervision.

Bingnan Li: writing—review and editing, data curation.

Lanzhi Wang: resources, data curation.

Zhenrong Gu: investigation. All authors contributed to the study conception and design.

Data availability The air pollutant data used during this study are from the NASA, and other datasets analyzed are available from the corresponding author on reasonable request.

Ethical Responsibilities of Authors "All authors have read, understood, and have complied as applicable with the statement on "Ethical responsibilities of Authors" as found in the Instructions for Authors".

Consent to Participate This paper does not require consent to participate.

Consent for Publication The first author and the responsible author agree to publish the paper.

References

[1] Li Lei, He Yuqing, Lan Zijuan, et al. Analysis of Environmental Meteorological Characteristics of Ozone Pollution in Shenzhen [J]. Journal of Environmental Science, 2023, 43 (01): 109-118. DOI: 10.13671/j.hjkxxb. 2022.0408

[2] Szep, R., Keresztes, R., Tonk, S., Korodi, A. & Craciun, M.E. (2017). The Examination of the Effects of Relative Humidity on the Changes of Tropospheric Ozone Concentrations in the Ciuc Basin, Romania. Revista de Chimie, 68(4), 642-645. https://doi.org/10.37358/RC.17.4.5522

[3] Cristofanelli, P., Bracci, A., Sprenger, M., Marinoni, A., Bonafè, U., Calzolari, F., Duchi, R., Laj, P., Pichon, J. M., Roccato, F., Venzac, H., Vuillermoz, E., & Bonasoni, P. (2010). Tropospheric ozone variations at the Nepal Climate Observatory-Pyramid (Himalayas, 5079 m a.s.l.) and influence of deep stratospheric intrusion events. Atmospheric Chemistry and Physics, 10(14), 6537-6549. https://doi.org/10.5194/acp-10-6537-2010

[4] Ziemke, J. R., Oman, L. D., Strode, S. A., Douglass, A. R., Olsen, M. A., McPeters, R. D., Bhartia, P. K., Froidevaux, L., Labow, G. J., Witte, J. C., Thompson, A. M., Haffner, D. P., Kramarova, N. A., Frith, S. M., Huang, L.-K., Jaross, G. R., Seftor, C. J., Deland, M. T., & Taylor, S. L. (2019). Trends in global tropospheric ozone inferred from a composite record of TOMS/OMI/MLS/OMPS satellite measurements and the MERRA-2 GMI simulation. Atmospheric Chemistry and Physics, 19(5), 3257-3269. https://doi.org/10.5194/acp-19-3257-2019

[5] Lelieveld, J., Proestos, Y., Hadjinicolaou, P., Tanarhte, M., Tyrlis, E., & Zittis, G. (2016). Strongly increasing heat extremes in the Middle East and North Africa (MENA) in the 21st century. Climatic Change, 137(1-2), 245-260. https://doi.org/10.1007/s10584-016-1665-6

[6] Tadic, I., Crowley, J. N., Dienhart, D., Eger, P., Harder, H., Hottmann, B., Martinez, M., Parchatka, U., Paris, J.-D., Pozzer, A., Rohloff, R., Schuladen, J., Shenolikar, J., Tauer, S., Lelieveld, J., & Fischer, H. (2020). Net ozone production and its relationship to nitrogen oxides and volatile organic compounds in the marine boundary layer around the Arabian Peninsula. Atmospheric Chemistry and Physics, 20(11), 6769-6787. https://doi.org/10.5194/acp-20-6769-2020

[7] Nadeem A, Tariq S, Haq ZU. Long-term quantification of springtime aerosols over Saudi Arabia using multi-satellite remotely sensed data. Environ Sci Pollut Res Int. 2024 Jun; 31(29):42023-42033. doi: 10.1007/s11356-024-33871-0. Epub 2024 Jun 10. PMID: 38856855.

[8] Al Suwaidi, A., Ali, T., Atabay, S. et al. Particulate matter (pm10) monitoring in the United Arab Emirates using a satellite remote sensing based model. Discov Environ 2, 50 (2024). https://doi.org/10.1007/s44274-024-00068-8

[9] Jiang, Z., Miyazaki, K., Worden, J. R., Liu, J. J., Jones, D. B. A., & Henze, D. K. (2016). Impacts of anthropogenic and natural sources on free tropospheric ozone over the Middle East. Atmospheric Chemistry and Physics, 16(10), 6537-6546. https://doi.org/10.5194/acp-16-6537-2016

[10] Badaro-Saliba, N., Adjizian-Gerard, J., Zaarour, R., Abboud, M., Farah, W., Saliba, A. N., & Shihadeh, A. (2013). A geostatistical approach for assessing population exposure to NO2 in a complex urban area (Beirut, Lebanon). Stochastic Environmental Research and Risk Assessment, 28(3), 467-474. https://doi.org/10.1007/s00477-013-0765-3

[11] Zohdirad, H., Montazeri Namin, M., Ashrafi, K., Aksoyoglu, S., & Prevot, A. S. H. (2022). Temporal

ISSN 2616-5872 Vol.6, Issue 5: 57-72, DOI: 10.25236/AJEE.2024.060509

variations, regional contribution, and cluster analyses of ozone and NO(x) in a middle eastern megacity during summertime over 2017-2019. Environ Sci Pollut Res Int, 29(11), 16233-16249. https://doi.org/10.1007/s11356-021-14923-1

[12] Daniel A. Jaffe, Owen R. Cooper, Arlene M. Fiore, Barron H. Henderson, Gail S. Tonnesen, Armistead G. Russell, Daven K. Henze, Andrew O. Langford, Meiyun Lin, Tom Moore; Scientific assessment of background ozone over the U.S.: Implications for air quality management. Elementa: Science of the Anthropocene 1 January 2018; 6 56. doi: https://doi.org/10.1525/elementa.309

[13] Abbasi-Kangevari, M., Malekpour, M. R., Masinaei, M., Moghaddam, S. S., Ghamari, S. H., Abbasi-Kangevari, Z., Rezaei, N., Rezaei, N., Mokdad, A. H., Naghavi, M., Larijani, B., Farzadfar, F., Murray, C. J. L., Africa, G. B. D. N., & the Middle East Air Pollution, C. (2023). Effect of air pollution on disease burden, mortality, and life expectancy in North Africa and the Middle East: a systematic analysis for the Global Burden of Disease Study 2019. Lancet Planet Health, 7(5), e358-e369. https://doi.org/10.1016/S2542-5196(23)00053-0

[14] Barkley, M. P., González Abad, G., Kurosu, T. P., Spurr, R., Torbatian, S., & Lerot, C. (2017). OMI air-quality monitoring over the Middle East. Atmospheric Chemistry and Physics, 17(7), 4687-4709. https://doi.org/10.5194/acp-17-4687-2017

[15] Wang, W., van der A, R., Ding, J., van Weele, M., & Cheng, T. (2021). Spatial and temporal changes of the ozone sensitivity in China based on satellite and ground-based observations. Atmospheric Chemistry and Physics, 21(9), 7253-7269. https://doi.org/10.5194/acp-21-7253-2021

[16] Peng, S., Ju, T., Liang, Z., Li, M., Liu, S., & Pan, B. (2022). Analysis of atmospheric ozone in Fenwei Plain based on remote sensing monitoring. Environ Monit Assess, 194(6), 412. https://doi.org/10.1007/s10661-022-10082-z

[17] Ting, M., Shaw, T. A., Seager, R., & Simpson, I. R. (2015). Mediterranean Summer Climate and the Importance of Middle East Topography. Journal of Climate, 28(5), 1977-1996. https://doi.org/10.1175/jcli-d-14-00298.1*

[18] Vrekoussis, M., Pikridas, M., Rousogenous, C., Christodoulou, A., Desservettaz, M., Sciare, J., Richter, A., Bougoudis, I., Savvides, C., & Papadopoulos, C. (2022). Local and regional air pollution characteristics in Cyprus: A long-term trace gases observations analysis. Sci Total Environ, 845, 157315. https://doi.org/10.1016/j.scitotenv.2022.157315

[19] Ehsan, M. A., Nicolì, D., Kucharski, F., Almazroui, M., Tippett, M. K., Bellucci, A., Ruggieri, P., & Kang, I.-S. (2020). Atlantic Ocean influence on Middle East summer surface air temperature. npj Climate and Atmospheric Science, 3(1). https://doi.org/10.1038/s41612-020-0109-1

[20] Osipov, S., Chowdhury, S., Crowley, J. N., Tadic, I., Drewnick, F., Borrmann, S., Eger, P., Fachinger, F., Fischer, H., Predybaylo, E., Fnais, M., Harder, H., Pikridas, M., Vouterakos, P., Pozzer, A., Sciare, J., Ukhov, A., Stenchikov, G. L., Williams, J., & Lelieveld, J. (2022). Severe atmospheric pollution in the Middle East is attributable to anthropogenic sources. Communications Earth & Environment, 3(1). https://doi.org/10.1038/s43247-022-00514-6

[21] Kalbarczyk, R., Kalbarczyk, E., Niedźwiecka-Filipiak, I., & Serafin, L. (2015). Ozone Concentration at Ground Level Depending on the Content of NOx and Meteorological Conditions. Ecological Chemistry and Engineering S, 22(4), 527-541. https://doi.org/10.1515/eces-2015-0031

[22] Xiong, Y., & Du, K. (2020). Source-resolved attribution of ground-level ozone formation potential from VOC emissions in Metropolitan Vancouver, BC. Sci Total Environ, 721, 137698. https://doi.org/10.1016/j.scitotenv.2020.137698

[23] Ghimire, S., Lebo, Z. J., Murphy, S., Rahimi, S., & Tran, T. (2023). Simulations of winter ozone in the Upper Green River basin, Wyoming, using WRF-Chem. Atmospheric Chemistry and Physics, 23(16), 9413-9438. https://doi.org/10.5194/acp-23-9413-2023

[24] Spohn, T. K., & Rappenglück, B. (2015). Tracking potential sources of peak ozone concentrations in the upper troposphere over the Arabian Gulf region. Atmospheric Environment, 101, 257-269. https://doi.org/10.1016/j.atmosenv.2014.11.026

[25] Waha, K., Krummenauer, L., Adams, S., Aich, V., Baarsch, F., Coumou, D., Fader, M., Hoff, H., Jobbins, G., Marcus, R., Mengel, M., Otto, I. M., Perrette, M., Rocha, M., Robinson, A., & Schleussner, C.-F. (2017). Climate change impacts in the Middle East and Northern Africa (MENA) region and their implications for vulnerable population groups. Regional Environmental Change, 17(6), 1623-1638. https://doi.org/10.1007/s10113-017-1144-2

[26] Tazeem, S. B., Ahmed, N., & Hussain, A. (2022). Spatio-temporal co-variability of air pollutants and meteorological variables over Haqel and Jeddah, Saudi Arabia. AtmÓsfera. https://doi.org/10.20937/atm.53100

[27] Saqer, R., Issa, S., & Saleous, N. (2024). Spatio-temporal characterization of PM10 concentration across Abu Dhabi Emirate (UAE). Heliyon, 10(12), e32812. https://doi.org/ 10.1016/j. heliyon.2024.e32812

ISSN 2616-5872 Vol.6, Issue 5: 57-72, DOI: 10.25236/AJEE.2024.060509

[28] Zhao, Z., Zhou, Z., Russo, A., Du, H., Xiang, J., Zhang, J., & Zhou, C. (2021). Impact of meteorological conditions at multiple scales on ozone concentration in the Yangtze River Delta. Environ Sci Pollut Res Int, 28(44), 62991-63007. https://doi.org/10.1007/s11356-021-15160-2

[29] Li, M., Yu, S., Chen, X., Li, Z., Zhang, Y., Wang, L., Liu, W., Li, P., Lichtfouse, E., Rosenfeld, D., & Seinfeld, J. H. (2021). Large scale control of surface ozone by relative humidity observed during warm seasons in China. Environmental Chemistry Letters, 19(6), 3981-3989. https://doi.org/10.1007/s10311-021-01265-0

[30] Kalabokas, P., Hjorth, J., Foret, G., Dufour, G., Eremenko, M., Siour, G., Cuesta, J., & Beekmann, M. (2017). An investigation on the origin of regional springtime ozone episodes in the western Mediterranean. Atmospheric Chemistry and Physics, 17(6), 3905-3928. https://doi.org/10.5194/acp-17-3905-2017